Inclusion of Crawl Tests and Long-Term Health Monitoring in Bridge Serviceability Analysis

André D. Orcesi[1] and Dan M. Frangopol[2]

Abstract: Due to limited resources, structural health monitoring (SHM) of highway bridges has to be integrated in structural performance assessment in a cost-effective manner. The instrumentation and the long-term SHM procedures are generally chosen with emphasis on most critical bridge components for a particular failure mode. However, global structural analysis is necessary to obtain useful structural performance information. It is then a major challenge to use monitoring data at some locations to perform a structural reliability analysis at other locations. In this paper, a methodology for lifetime serviceability analysis of existing steel girder bridges including crawl tests and long-term monitoring information is presented. The case where the initial goal of monitoring is to provide data for a fatigue analysis of some bridge components is considered. The monitoring results are used to perform a structural reliability analysis of different sections that are critical considering serviceability of the bridge. Limit state equations are used firstly by adhering to the load and strength formulas and requirements set forth in AASHTO specifications, and secondly by integrating monitoring information. Serviceability with respect to permanent deformation under overload is estimated for the girders with these two different methods and a time-dependent performance analysis is conducted by considering corrosion penetration. The proposed approach is applied to the I-39 Northbound Bridge over the Wisconsin River in Wisconsin. A monitoring program of that bridge was performed by the Advanced Technology for Large Structural Systems Center at Lehigh University.

DOI: 10.1061/(ASCE)BE.1943-5592.0000060

CE Database subject headings: Structural reliability; Monitoring; Serviceability; Bridges.

Author keywords: Structural health monitoring; Crawl test; Long-term monitoring; Serviceability; Reliability.

Introduction

One common issue in civil infrastructure systems is the need to monitor, assess, and predict structural integrity and durability of structural systems and their various components (Ang and De Leon 2005; Ellingwood 2005). Structural health monitoring (SHM) provides a powerful and needed tool to reduce uncertainty, calibrate, and improve structural assessment and performance prediction models (Hess 2007; Frangopol and Liu 2007; Frangopol and Messervey 2009b). The monitoring cost naturally represents a constraint and instrumentation is generally conducted to update the performance knowledge of some particular components of the bridge. The monitoring data are, therefore, generally related to only a few components of the structure. The main disadvantage is that sensors are only able to provide data that are representative of the conditions at the sensor locations (Marsh and Frangopol 2007). When possible, it is of interest to extend the initial purpose of the monitoring process and conduct structural analysis at some other locations of the bridge that can be critical concerning different failure modes. Moreover, the inclusion of SHM in life-cycle costs analysis still represents a challenge, and there is a strong need in developing a general framework to update life-cycle cost analysis with monitoring data (Frangopol et al. 2008a).

This paper presents a probabilistic framework that can be used for forecasting the serviceability lifetime performance of existing steel girder bridges. The main objective is to show how to integrate monitoring data obtained at some particular locations in a general reliability analysis. The I-39 Northbound Bridge, over the Wisconsin River, long-term monitored by the National Center for Advanced Technology for Large Structural Systems (ATLSS), at Lehigh University, Bethlehem, Pa. (Mahmoud et al. 2005) offers the opportunity to perform studies including monitoring results in a global reliability analysis. A fatigue analysis of various fatigue prone details was performed to assess their fatigue remaining life. The instrumentation consisted of installation of weldable resistance strain gauges at key locations to understand the response of the bridge to loads and quantify the stress-range histograms at critical details. The main goal of the monitoring tests on the I-39 bridge was to perform a fatigue analysis at some local details of the steel girders. Therefore, sensors were placed at the critical locations concerning fatigue (e.g., connection between girders). However, the fatigue critical locations might not be critical concerning structural capacity of the bridge.

First, this study proposes to use monitoring data obtained at the sensor locations to assess traffic effect in different components of the structure. SHM methodologies generally require accurate and practical structural models to compare obtained

[1]Research Associate, Laboratoire Central des Ponts et Chaussées, Section Durabilité des Ouvrages d'Art, Division Fonctionnement et Durabilité des Ouvrages d'Art, 58 Blvd. Lefebvre, F-75732 Paris Cedex 15, France. E-mail: andre.orcesi@lcpc.fr

[2]Professor and The Fazlur R. Kahn Endowed Chair of Structural Engineering and Architecture, Dept. of Civil and Environmental Engineering, ATLSS Center, Lehigh Univ., 117 ATLSS Dr., Bethlehem, PA 18015-4729 (corresponding author). E-mail: dan.frangopol@lehigh.edu

Note. This manuscript was submitted on April 10, 2009; approved on July 29, 2009; published online on April 15, 2010. Discussion period open until October 1, 2010; separate discussions must be submitted for individual papers. This paper is part of the ***Journal of Bridge Engineering***, Vol. 15, No. 3, May 1, 2010. ©ASCE, ISSN 1084-0702/2010/3-312–326/$25.00.

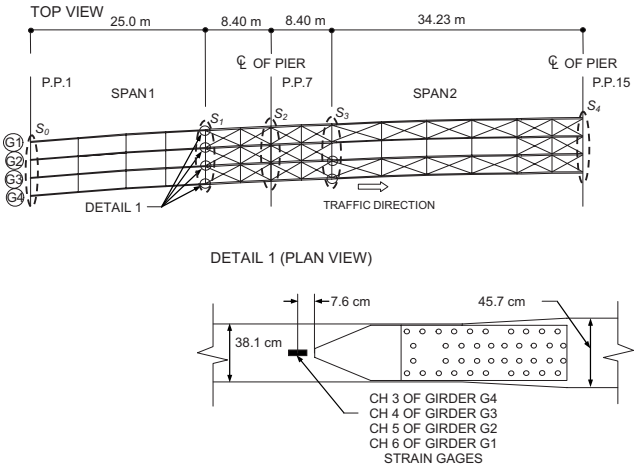

Fig. 1. Sensor Locations on the I-39 Northbound Wisconsin River Bridge (adapted from Mahmoud et al. 2005)

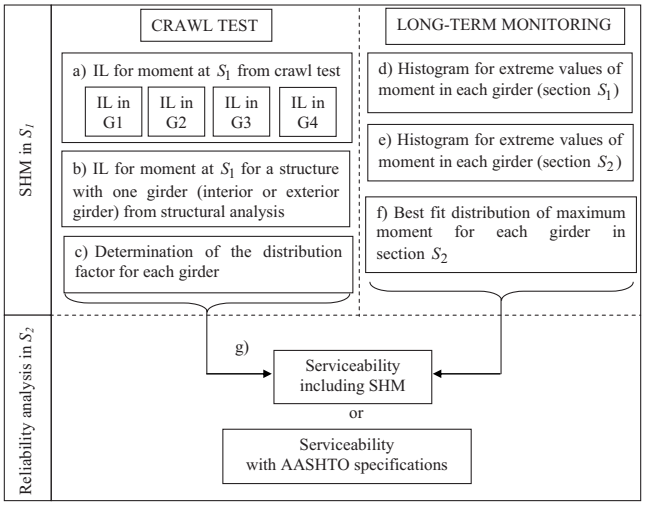

Fig. 2. Steps of the proposed methodology

information with modeled structural behavior. The determination of numerical models that are able to describe accurately the static and dynamic response of bridges has been largely investigated and several numerical methods to model structures have already been proposed (Douglas and Reid 1982; Aktan et al. 1997, 1998; Morassi and Tonon 2008). The objective is herein to compare in situ information obtained with controlled load tests with a practical numerical model to identify distribution of live loads in the structure. Second, a reliability analysis is performed at critical sections for structural capacity including or not including the monitoring information. Analysis results are presented in terms of the initial reliability indices and lifetime reliability profiles. The aim is to show that some data obtained at one location can be successfully used at a different location.

Methodology

As indicated previously, the proposed methodology is applied to the I-39 Northbound Bridge, over the Wisconsin River, long-term monitored by the National Center for ATLSS, at Lehigh University, Bethlehem Pa. The study focuses on the monitored data from Channels 3, 4, 5, and 6 (denoted as CH3, CH4, CH5, and CH6, respectively) of the I-39 Bridge (see Fig. 1) which measured and recorded the structural responses of the east exterior girder (G4), east interior girder (G3), west interior girder (G2), and west exterior girder (G1), respectively (Fig. 1). The corresponding sensors were installed at the bottoms of the bottom flanges in the section S_1 (Fig. 1), which is located about 25.0m north of the central line of the south abutment of the bridge. The proposed methodology uses data obtained during crawl tests and long-term monitoring at sensor locations to perform a structural reliability analysis in section S_2, which is at the pier between spans 1 and 2 of the bridge (Fig. 1), and where negative flexural moments due to dead loads are significant. The general steps are illustrated in Fig. 2 and each step is detailed below:

1. Crawl test results are used to determine the influence line (IL) for the bending moment at sensor locations (section S_1). The ILs are determined from the crawl test for each girder i (and denoted as $\mathrm{IL}^{i}_{\mathrm{ct}(s_1)}$) for a vehicle in the left or in the right lane;
2. One girder of the bridge is modeled with a finite-element model and the IL, IL_{s_1}, for moment (denoted as $\mathrm{IL}^{\mathrm{int}}_{s_1}$ for an interior girder and $\mathrm{IL}^{\mathrm{ext}}_{s_1}$ for an exterior girder) is calculated for this girder at the section S_1;
3. The comparison of $\mathrm{IL}^{i}_{\mathrm{ct}(s_1)}$ with IL_{s_1} allows to assess the distribution factor (DF) for each girder i when the vehicle is in the left or the right lane;
4. Long-term monitoring provides a histogram of bending moment in each girder (in section S_1);
5. The IL for moment IL_{s_2} is calculated for section S_2 (Fig. 1). This IL is denoted as $\mathrm{IL}^{\mathrm{int}}_{s_2}$ and $\mathrm{IL}^{\mathrm{ext}}_{s_2}$ for interior and exterior girders, respectively. Ratios r_{int} and r_{ext}, between the peak values of $\mathrm{IL}^{\mathrm{int}}_{s_1}$ and $\mathrm{IL}^{\mathrm{int}}_{s_2}$ and those of $\mathrm{IL}^{\mathrm{ext}}_{s_1}$ and $\mathrm{IL}^{\mathrm{ext}}_{s_2}$, are determined, respectively. These ratios enable to determine the histograms for moment in section S_2 from those in section S_1 by considering that the traffic has the same spatial distribution in sections S_1 and S_2;
6. Best fit distributions of maximum moment induced by trucks can be determined in section S_2 for each girder; and
7. Serviceability limit state equations dealing with the resistance moment in girders and the maximum moment produced by heavy trucks are introduced. Limit state equations are derived either by strictly adhering to the load and capacity formulas and requirements set forth in AASHTO (2007) specifications, or by integrating monitoring results (updating of DFs and use of best fit distributions in the limit state equation). Reliability indices with respect to serviceability of components are calculated for the girders (the deck serviceability is not analyzed in this study) using these two different methods and a time-dependent performance analysis is conducted by considering corrosion penetration.

SHM is used in two different ways to update the reliability analysis (Fig. 2). On one hand, crawl tests results are used to determine in situ DFs for each girder when trucks are in different lanes. On the other hand, long-term monitoring results are used to approach the extreme moment due to heavy trucks and determine the probability that this extreme moment is larger than the moment capacity of each girder.

Use of IL in Reliability Analysis

Determination of the IL for Each Girder Using Crawl Tests

For a crawl test with moving load monitoring, a truck loaded with identified weight moves along a predetermined path (usually, traffic lanes) across the bridge at a steady speed. The ILs for a given load effect, such as a reaction, axial force, shear force, or bending moment, can be determined using the methodology proposed by O'Brien et al. (2006). It enables to derive the IL from direct measurements of the load effect in response to a multiwheel vehicle of known weight. Introducing some parameters such as the scanning frequency f of data acquisition unit, the speed v of the vehicle, the number N of axles of the vehicle, and the distance D_i between axle i and the first axle of the vehicle, the method compares the theoretical effect of the vehicle in kth scan with the one that is measured in sensors. The theoretical effect is (O'Brien et al. 2006)

$$L_k^T = \sum_{i=1}^{N} A_i \tilde{I}_{(k-C_i)} \tag{1}$$

where $\tilde{I}$=influence ordinate; A_i=weight of the ith axle; and C_i =number of scans ($C_i = D_i f / v$). An error function equal to the sum of the squares of the differences between the measured, L_k^M, and theoretical, L_k^T, load effects for the K scans is defined as (Moses 1979)

$$E = \sum_{k=1}^{K} (L_k^M - L_k^T)^2 \tag{2}$$

The set of influence ordinates is then found by minimizing the error E. The Rth influence ordinates, $\tilde{I}_R$, is the one for which $\partial E / \partial \tilde{I}_R = 0$. Setting all partial derivatives to zero gives a set of $K - C_N$ simultaneous equations expressed as $\boldsymbol{W}\tilde{\boldsymbol{I}} = \varepsilon$, where $\boldsymbol{W}$ is a sparse symmetric matrix dependent on the vehicle axle weights, $\tilde{\boldsymbol{I}}$ is a vector of sought influence ordinates, and ε is a vector dependent on the vehicle axle weights and the measured load effect readings. For a truck with three axles, the diagonal elements of matrix $\boldsymbol{W}$ are $w_{ii} = \Sigma_{i=1}^{N} A_i^2$, and the nonzero upper triangular elements are expressed as $w_{i+(C_3-C_2)} = A_2 A_3$, $w_{i+C_2} = A_1 A_2$, and $w_{i+C_3} = A_1 A_3$ (see O'Brien et al. 2006 for details). For a truck with three axles, the vector ε is expressed as follows:

$$\varepsilon = \begin{pmatrix} A_1 L_1^M + A_2 L_{1+C_2}^M + A_3 L_{1+C_3}^M \\ A_1 L_2^M + A_2 L_{2+C_2}^M + A_3 L_{2+C_3}^M \\ A_1 L_3^M + A_2 L_{3+C_2}^M + A_3 L_{3+C_3}^M \\ \vdots \\ A_1 L_{K-C_3}^M + A_2 L_{K+C_2}^M + A_3 L_K^M \end{pmatrix} \tag{3}$$

Finally, the vector $\tilde{\boldsymbol{I}}$ of influence ordinates can be obtained by inverting the square matrix $\boldsymbol{W}$, or by Cholesky factorization (the $\boldsymbol{W}$ matrix is symmetric positive definite).

Determination of the IL by Modeling the Bridge

One girder of the multispan I-39 Bridge is also modeled, using finite elements (SAP 2000 2009). Its cross section is shown in Fig. 3 (descriptions of parameters are provided in Tables 1 and 2).

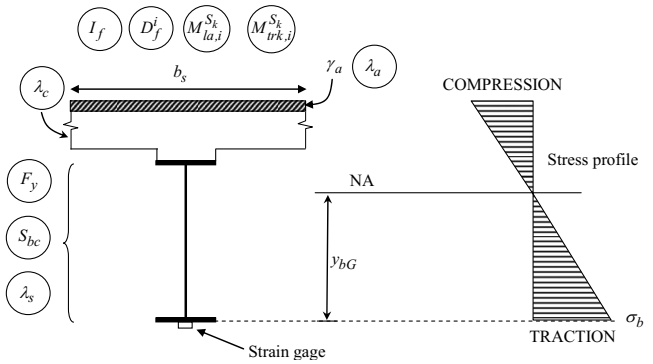

Fig. 3. Deterministic parameters and selected random variables (circled) for the steel bridge girder [adapted from Akgül and Frangopol (2004)]

It is noted that frame elements are used to model the girder and that ideal support conditions (hinged supports) are considered to fix the degrees of freedom. Due to the presence of composite and noncomposite sections, and to the variation in the dimensions of the sections, several section types are identified (see Fig. 4 for identified sections in span 1 of I-39 Bridge) and the associated moments of inertia are provided in Table 3. Slab contribution for composite sections (where concrete is in compression) is considered by converting the concrete area into an equivalent steel girder area. For one girder, the area of concrete, obtained by considering the effective slab width b_s, is different for interior and exterior girders (AASHTO 2007). The overall structure is finally meshed to take into account the change of inertia of the girder between sections at midspan and at the pier, as explained previously. The IL for a given load effect, such as reaction, axial force, shear force, or bending moment, is generated for one girder (interior or exterior) by independently applying a unit load at several points on the considered structure and determining the value of the load effect at the desired location. As mentioned previously, the calculated ILs are denoted $\text{IL}_{s_1}^{\text{int}}$ and $\text{IL}_{s_1}^{\text{ext}}$ for an interior and exterior girder in section S_1, respectively, and $\text{IL}_{s_2}^{\text{int}}$ and $\text{IL}_{s_2}^{\text{ext}}$ for an interior and exterior girder in section S_2, respectively.

Comparison of ILs for Moment Obtained from Crawl Tests and from Calculations

For the I-39 Bridge, methodologies described previously are used to determine the influence line for the moment in section S_1, by using either crawl tests ($\text{IL}_{\text{ct}(s_1)}^{i}$), or structural analysis (IL_{s_1}). The truck considered herein has three main axles (i.e., one front axle and two rear axles) and two floating axles. The weights of the front axle and rear axles are 67.702 kN and 264.224 kN, respectively. This truck is used with a speed of 8 km/h traveling in the left or right lane [see Mahmoud et al. (2005) for a detailed overview of the crawl tests conducted on I-39 Bridge]. The monitoring of the structural response to the moving truck load is performed through strain measurements at sensor locations. Strain is converted to stress using Hooke's law. Figs. 5(c and d) show the response with time of CH3 through CH6 installed as the test truck passes over the right lane [see Fig. 5(a)] and the left lane [see Fig. 5(b)] in the crawl test, respectively. In all tests, the trucks travel northbound and the crawl tests start at the south abutment (section S_0). As illustrated in Fig. 5(c), high stress ranges are recorded in CH3 and CH4 when the truck is in the right lane. The remaining channels CH5 and CH6 also experience

Table 1. Random Variables for Steel Bridge Girder (All Random Variables Are Assumed to Have Lognormal Distribution; Each Random Variable Is Characterized by Its Mean Value μ and Standard Deviation σ)

Random variable	Description	μ	σ
F_y [a] (MPa)	Yield strength of steel girder (MPa)	344.73	41.36
λ_a [b]	Asphalt weight uncertainty factor	1	0.25
λ_c [b]	Concrete weight uncertainty factor	1.05	0.105
λ_s [b]	Structural steel weight uncertainty factor	1.03	0.0824
S_{bc}(cm^3)	Elastic section modulus (cm^3)	Varies with time	Varies with time
$M_{la,i}^{S_k}$(kN·m)	Moment associated with one design lane load in section S_k [see Fig. 12(b)]	Dependent on the section	Dependent on the section
$M_{trk,i}^{S_k}$(kN·m)	Moment associated with two design trucks in section S_k [see Fig. 12(c)]	1,421	568.7
I_f	Impact factor	1.33	0.133
D_f^i	DF (for girder G_i)	D_f^{Gi}	0.10 D_f^{Gi}

[a]Frangopol et al. (2008b).

[b]Akgül and Frangopol (2004).

high magnitude of stress-range cycles during the controlled load tests when test truck passes over the left lane [Fig. 5(d)]. The elastic moment in section S_1 is $M=\sigma_b I_1/y_{bG}$, where σ_b is the stress at the bottom flange of the girder, I_1 is the moment of inertia of the composite section S_1 (this inertia depends on the effective slab width b_s that is different for interior and exterior girders, see Figs. 3 and 4 and Table 3), and y_{bG} is the distance between elastic neutral axis and the bottom of the flange of the girder (also different for interior and exterior girders, see Fig. 3). The IL (for the structure with one girder), denoted IL_{s_1}, is calculated by structural analysis at section S_1 ($\mathrm{IL}_{s_1}^{\mathrm{int}}$ and $\mathrm{IL}_{s_1}^{\mathrm{ext}}$) by modeling one girder of the bridge with SAP 2000 (2009), when considering interior and exterior girders, respectively. For each girder i, the IL obtained with crawl tests ($\mathrm{IL}_{\mathrm{ct}(s_1)}^i$) is compared with IL_{s_1} ($\mathrm{IL}_{s_1}^{\mathrm{int}}$ or $\mathrm{IL}_{s_1}^{\mathrm{ext}}$) multiplied by a weighting factor γ_i (the resulting IL is denoted $\gamma_i \times \mathrm{IL}_{s_1}$). DF is usually assessed in AASHTO specifications. It depends on the number of lanes loaded and is different for exterior and interior girders. This factor also includes the probability of simultaneous lane occupation through the use of a multiple presence factor m. However, some uncertainties are linked to the calculation of these DFs and it is of interest to calibrate them with in situ information. DFs can be assessed herein in three steps: first by determining γ_i such that the peaks of $\mathrm{IL}_{\mathrm{ct}(s_1)}^i$ and $\gamma_i \times \mathrm{IL}_{s_1}$ match in section S_1 (γ_i is denoted $\gamma_{i,r}$ when the truck is in the right lane and $\gamma_{i,l}$ when it is in the left lane); second by choosing γ_i as $\max(\gamma_{i,r}, \gamma_{i,l})$; and third by multiplying γ_i with the multiple presence factor m, as defined in AASHTO (2007), to obtain the DF for each girder.

Comparison of influence line for moment obtained by calculations and by the crawl test, for sensors CH3, CH4, CH5, and CH6, when the truck is in the right lane, is shown in Figs. 6(a–d), respectively. For a truck in the right lane, the weighting factor $\gamma_{i,r}$ is 0.43, 0.47, 0.25, and 0.15 for the girders G4, G3, G2, and G1, respectively. Using $\gamma_{i,r}$ for each girder i, it can be seen that the IL, $\mathrm{IL}_{\mathrm{ct}(s_1)}^i$, found with crawl test, and $\gamma_{i,r} \times \mathrm{IL}_{s_1}$ are very close. It is noted that there is a slight difference between ILs for girder G3 when the load is at midspan [see Fig. 6(b)], the ordinate of the measured IL being lower than that of the modeled one. However, this error is conservative since the absolute value $\gamma_{i,r} \times \mathrm{IL}_{s_1}$ is always equal or larger than the absolute value of the $\mathrm{IL}_{\mathrm{ct}(s_1)}^i$, for each girder i. When the truck is in the left lane, the weighting factor $\gamma_{i,l}$ that enables to match crawl test $\mathrm{IL}_{\mathrm{ct}(s_1)}^i$ and $\gamma_{i,l} \times \mathrm{IL}_{s_1}$ at section S_1 is 0.12, 0.25, 0.47, and 0.45 for girders G4, G3, G2, and G1, respectively (see Fig. 7).

Finally, the weighting factor for each girder γ_i (associated with the worst case of loading) is $\max(\gamma_{i,r}, \gamma_{i,l})$. Therefore, for the four girders of the I-39 Bridge, γ_i=0.43, 0.47, 0.47, and 0.45 for girders G4, G3, G2, and G1, respectively. As explained previously, the extreme live load effect needs to be determined by considering each possible combination of number of loaded lanes multiplied by a corresponding multiple presence factor to account for the probability of simultaneous lane occupation. For one lane loaded, this coefficient is m=1.2. The coefficient γ_i, obtained previously, is multiplied by this coefficient and the DF is finally 0.52, 0.56, 0.56, and 0.54 for girders G4, G3, G2, and G1, respectively.

Table 2. Deterministic Parameters for Steel Bridge Girder

Deterministic parameter	Description	Value
γ_a [a]	Unit weight of asphalt pavement (kN/m^3)	22.73
t_a	Thickness of asphalt pavement (cm)	8.9
t_s	Thickness of concrete slab (cm)	19
L	Length of the span if the region is in positive flexure and average of the length of the two adjacent spans if the region is in negative flexure (m)	Varies see Eq. (9)
N_G	Number of girders	4

[a]Akgül and Frangopol (2004).

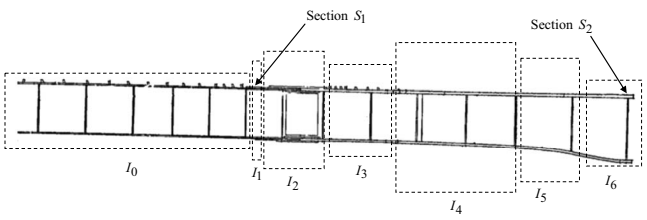

Fig. 4. Moments of inertia considered in the different sections of span 1 of I-39 Bridge

Table 3. Moments of Inertia for Sections of Span 1 (See Fig. 4)

Moment of inertia ($\times 10^{10}$ mm^4)	Interior girder	Exterior girder
I_0 (composite section)	2.1070	1.7654
I_1 (composite section)	2.9684	2.4743
I_2 (composite section)	3.3748	2.8443
I_3 (non composite section)	2.4916	2.4916
I_4 (non composite section)	2.8750	2.8750
I_5 (non composite section)	3.3979	3.3979
I_6 (non composite section)	3.9704	3.9704

Analysis of Long-Term Monitoring Results

Statistics of Extremes

In this study, the predictions of future component and system reliabilities are based on the statistics of extremes (extreme values are understood as largest values of a random variable herein). In a set of observations (e.g., SHM data), extreme values can be modeled as random variables. When the number of SHM data, k, is large enough, the extreme value distribution of the SHM data will asymptotically approach one of the following three probability distributions: (a) Gumbel distribution; (b) Fisher-Tippett distribution; and (c) Weibull distribution, regardless of the original probability distributions of the SHM data (Ang and Tang 1984). The Gumbel probability distribution (Gumbel 1958)

$$F(M_\chi) = \exp\left[-\exp\left(-\frac{M_\chi - \lambda}{\eta}\right)\right] \tag{4}$$

is adopted herein, where $F(M_\chi)$=cumulative distribution function of the Gumbel probability distribution; M_χ=extreme value of a random variable M [i.e., the maximum value of $M_i(i=1,\ldots,k)$]; λ=location parameter; and η=scale parameter to be determined from the measured data by using theory of order statistics.

Long-term Monitoring Program

The monitored strain data from the uncontrolled load tests (under each of the passages of the heavy vehicle traffics) were extensively collected and investigated during the period from August 12 to November 3, 2004 (denoted as period T_1). It is reminded that all the monitored strain data used in this study are converted into stress data under the assumption that these strain data follow the Hooke's law, and then in moment. In order to minimize the volume of monitoring data and to consider only the heavy vehicles, recording of the data in Channels CH3, CH4, CH5, and CH6 was triggered when the vehicle induced the strain larger than the predefined strain (Mahmoud et al. 2005). 716 events were captured during the monitoring period T_1, of which 510 heavy vehicles crossed the bridge on the right (east) lane and 210 heavy vehicles crossed the bridge on the left (west) lane.

As explained in Fig. 2, the objective is to lead a reliability analysis in section S_2 whereas results are found in section S_1. To

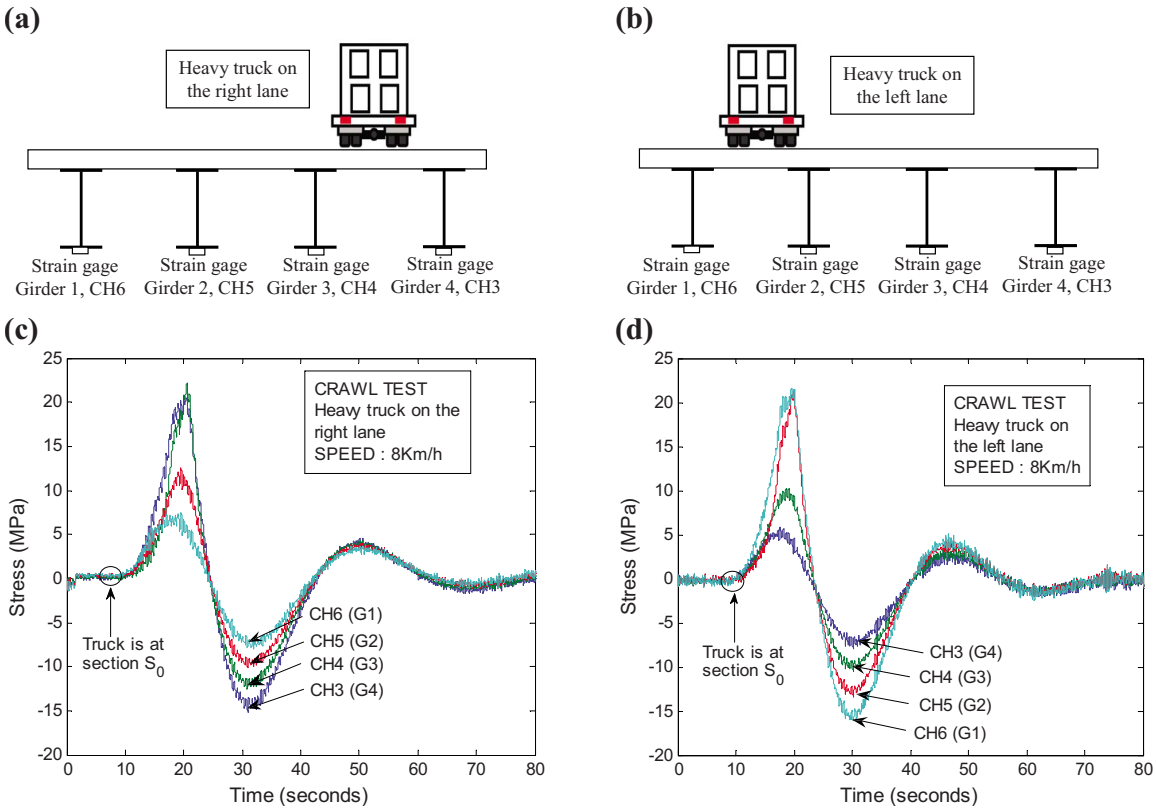

Fig. 5. Test truck starting at section S_0 (see Fig. 1) and passing (a) over the right lane in the crawl test; (b) over the left lane in the crawl test; responses of CH3 through CH6 installed in span 1 on girders G4 through G1, respectively (on the bottom face of the flange near welded cover plates) for a truck; (c) on the right lane; and (d) on the left lane [results based on data from Mahmoud et al. (2005)]

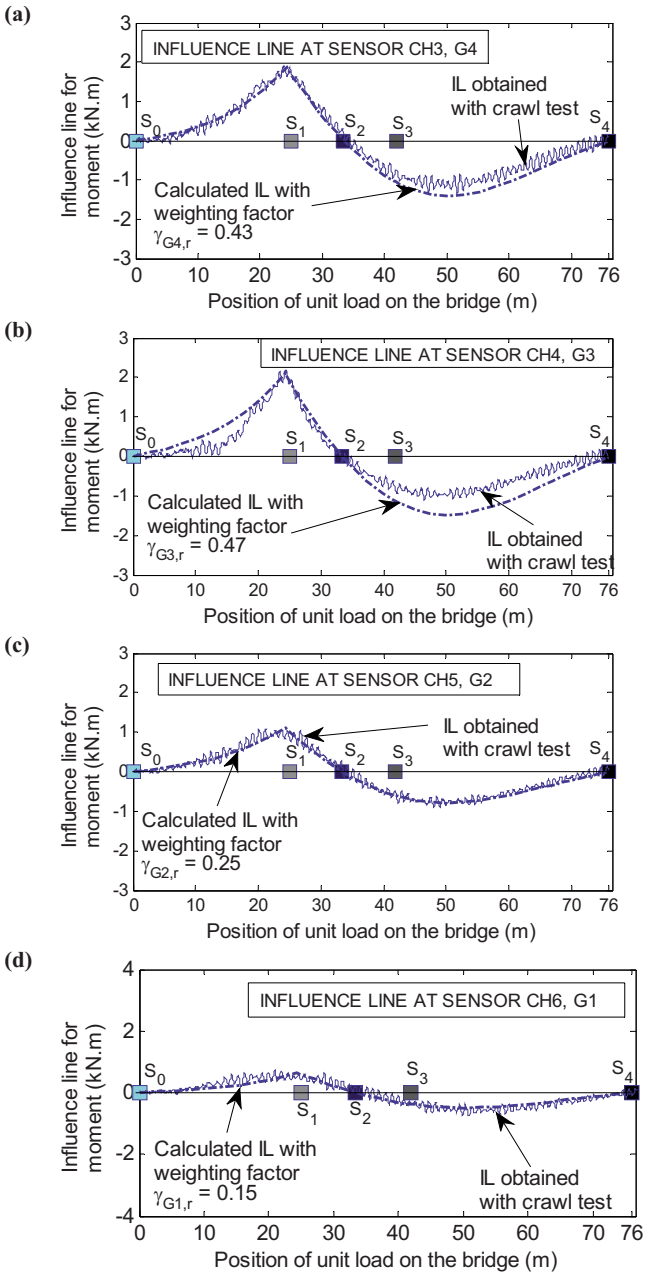

Fig. 6. IL (position of unit load is 0 when the load is at section S_0) obtained with crawl test (heavy truck on the right lane) and calculated IL weighted by the DF in channel: (a) CH3; (b) CH4; (c) CH5; and (d) CH6

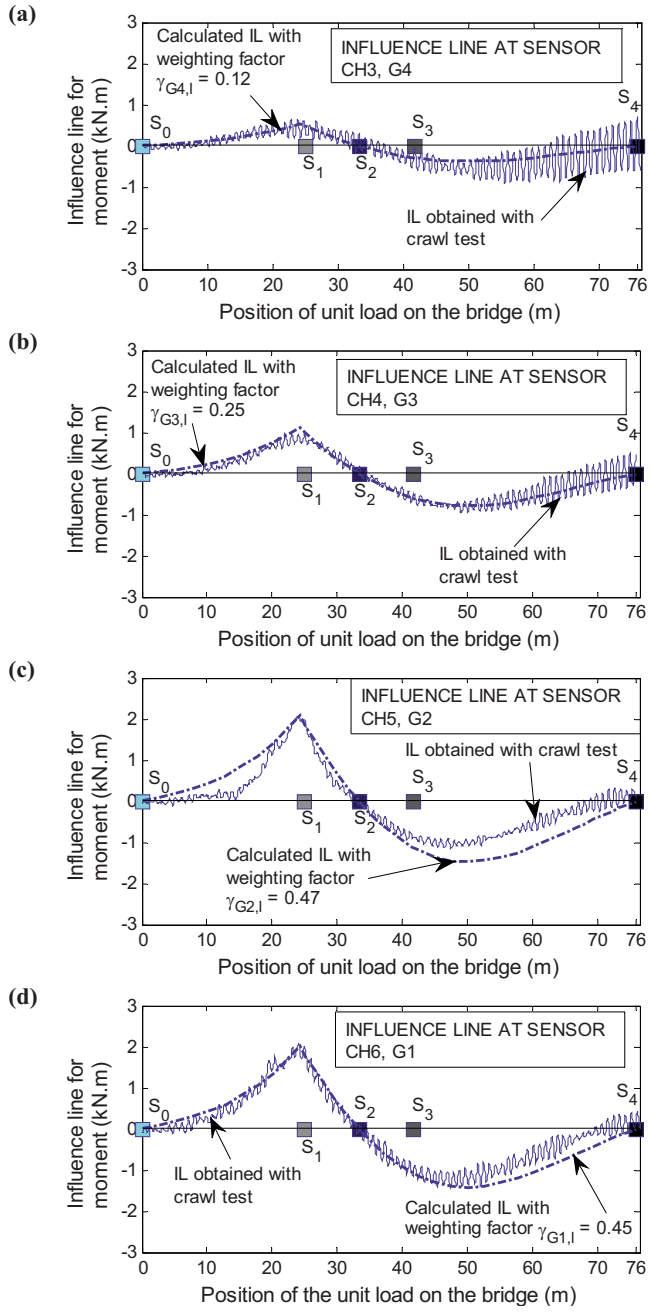

Fig. 7. IL (position of unit load is 0 when the load is at section S_0) obtained with crawl test (heavy truck on the left lane) and calculated IL weighted by the DF in channel: (a) CH3; (b) CH4; (c) CH5; and (d) CH6

lead the statistical analysis introduced above, histograms of moment in section S_2 need to be computed for each of the four girders G1, G2, G3, and G4.

ILs calculated for sections S_1 ($IL_{s_1}^{int}$ and $IL_{s_1}^{ext}$) and S_2 ($IL_{s_2}^{int}$ and $IL_{s_2}^{ext}$) are compared [Figs. 8(a and b)] when considering interior and exterior girders, respectively. For an interior girder, the ratio between the maximum absolute values of $IL_{s_2}^{int}$ and $IL_{s_1}^{int}$, denoted as $i_{2,int}$ and $i_{1,int}$, respectively [see Fig. 8(a)], is called r_{int} and is equal to $|i_{2,int}/i_{1,int}|$. The ratio $r_{ext}=|i_{2,ext}/i_{1,ext}|$ is determined in a similar way for an exterior girder [see Fig. 8(b)]. The histograms of the extreme moment are then assessed in section S_2 by simply multiplying the moment in section S_1 by the ratio r_{int} or r_{ext}, for an interior or exterior girder. It is assumed that the traffic distribution will not dramatically change between section S_1 and the section in which $IL_{s_2}^{int}$ and $IL_{s_2}^{ext}$ are equal to $i_{2,int}$ and $i_{2,ext}$ (Fig. 8). In other terms, trucks will be on the same lane when moving through the bridge between these two sections. Obviously, this assumption is meaningful only if the section of interest is not too far from the section that is instrumented, which is the case herein (Fig. 1).

The example that illustrates how to move from moment histogram in section S_1 [Fig. 9(a)] to moment histogram in section S_2 [Fig. 9(b)] is provided, considering channel CH3 if trucks are on the right lane. Distribution fitting is used for selecting the most appropriate distribution which fits to monitored data. Anderson-

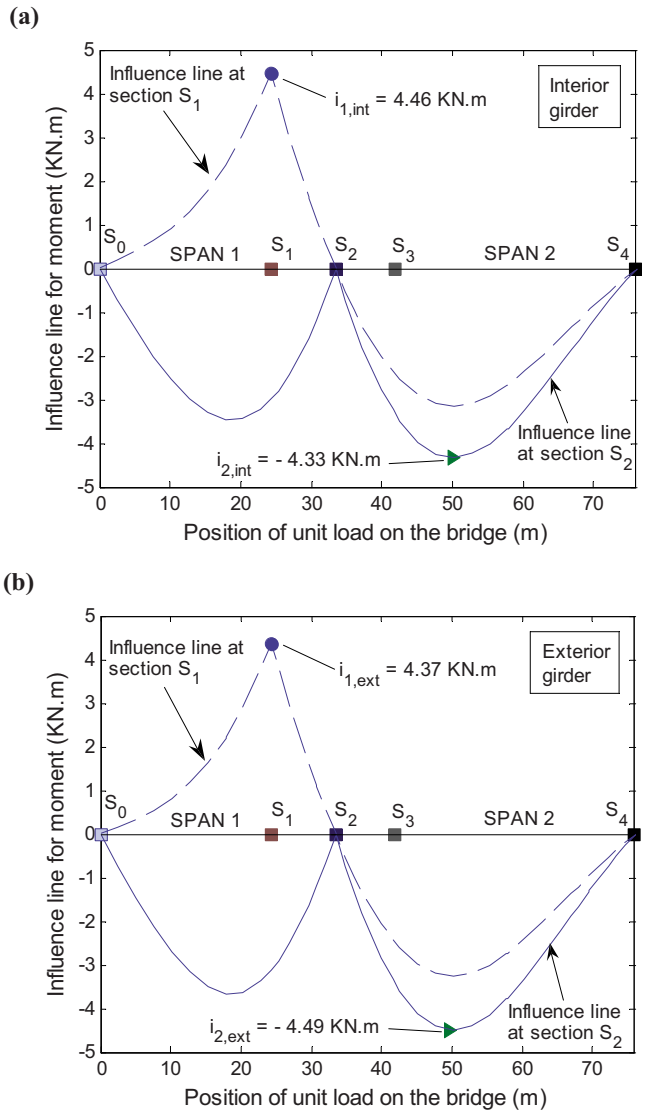

Fig. 8. IL obtained by structural analysis at sections S_1 and S_2 considering: (a) an interior girder ($IL_{s_1}^{int}$ at S_1 and $IL_{s_2}^{int}$ at S_2); (b) an exterior girder ($IL_{s_1}^{ext}$ at S_1 and $IL_{s_2}^{ext}$ at S_2)

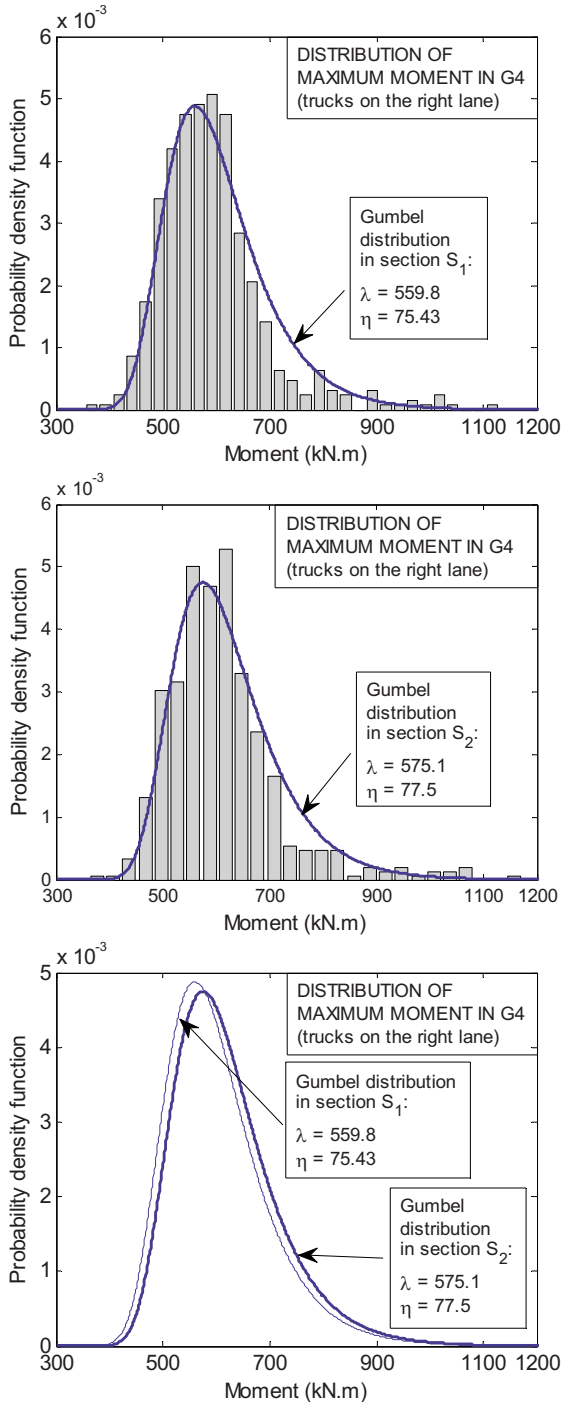

Fig. 9. (a) Histogram of monitored data in section S_1 for girder G4 and best fit distribution; (b) assessed histogram and best fit distribution in section S_2 for girder G4 obtained using histogram in section S_1 and the ratio $r_{ext}=|i_{2,ext}/i_{1,ext}|$; and (c) superposition of best-fit distributions for girder G4 in section S_1 and S_2

Darling test (Anderson and Darling 1952), which assigns more weight on the tail of a specific distribution than other tests (e.g., the Chi-square test or Kolmogorov-Smirnov test), was performed using MINITAB release 15 statistical software (2007). The Gumbel probability distribution function (PDF) was found to provide the best fittings to the histograms obtained from the monitored maximum moment (good results were also obtained for the log-normal PDF). Considering the example of channel CH3 when trucks are on the right lane, the best fitting values of the Gumbel distribution introduced in Eq. (4) are shown in Fig. 9(a) for section S_1, in Fig. 9(b) for section S_2, and are compared for these two sections in Fig. 9(c). In each case, the location and scale parameters are provided. All the histograms of moment are then computed in section S_2 for the four girders G4, G3, G2, and G1, when trucks are on the right lane (Fig. 10) and when they are on the left lane (Fig. 11). In each case, the solid line shows the best fitting values of the Gumbel distribution and the location and scale parameters are provided.

Serviceability Analysis

A serviceability analysis is investigated herein in the section S_2 at the pier (Fig. 1). As explained previously, the instrumentation of the bridge is generally influenced by a few initial objectives. In case of the I-39 Wisconsin Bridge, it is reminded that the main objective was to perform a complete fatigue analysis of the bridge and sensors were consequently placed at details that are critical

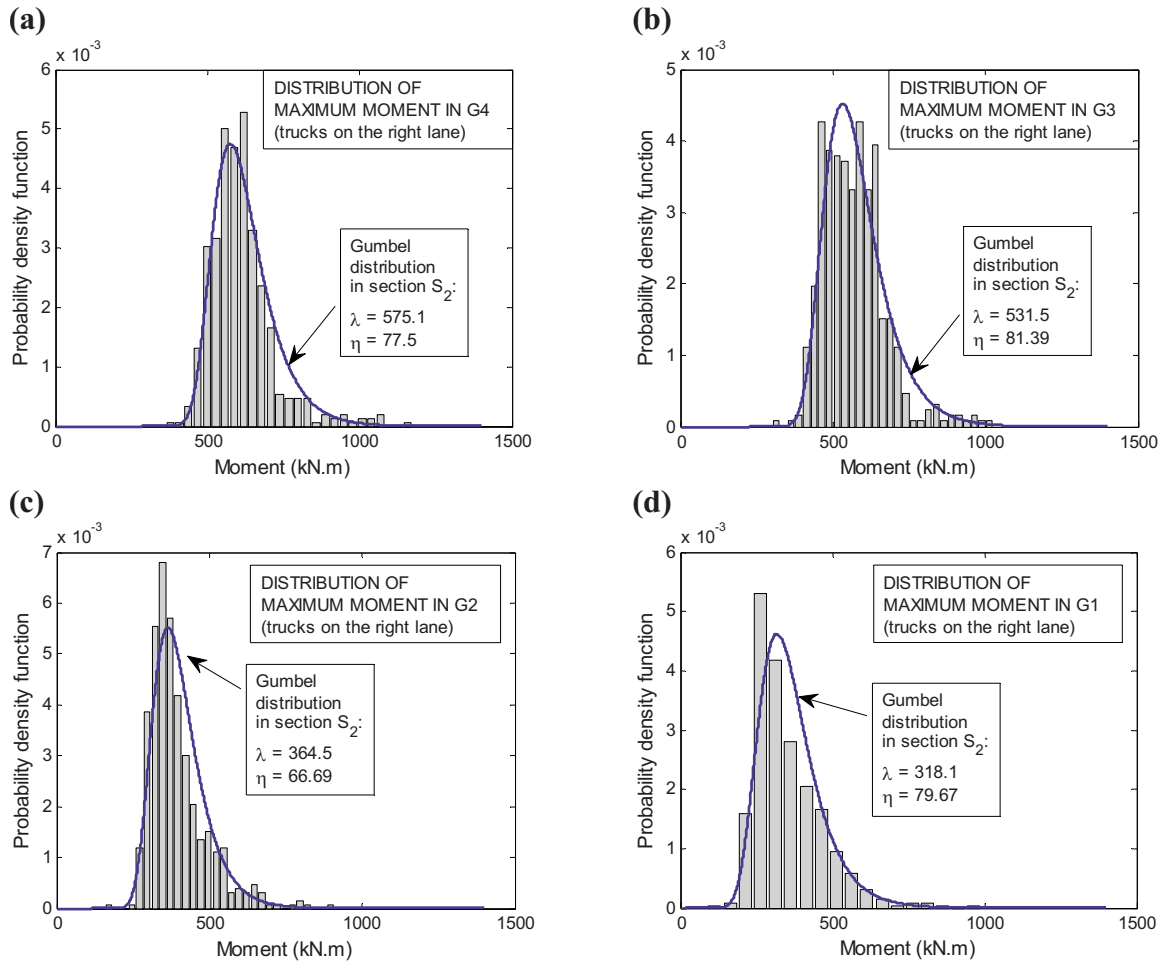

Fig. 10. Distribution of maximum moment in section S_2 (for trucks on the right lane) in: (a) G4; (b) G3; (c) G2; and (d) G1

for fatigue (like connections between two girders for example) but not necessarily for structural capacity. Fig. 12(a) shows the bending moment in exterior and interior girders due to composite (denoted $M_{\mathrm{DLC},i}$) and noncomposite (denoted $M_{\mathrm{DLNC},i}$) dead loads in the two first spans of the I-39 Bridge (these moments are detailed in the following section). From this figure, it is obvious that sensors are in a location where the moment due to dead loads is very close to 0 (section S_1). Indeed, these sensors are at a connection between two girders and those connections are often located where the moment due to dead loads is very low. However, this moment has very high values in section S_2 (see Fig. 12), which justifies to perform the reliability analysis in this section. A reliability analysis using the RELSYS (RELiability of SYStems) computer program developed at the University of Colorado (Estes and Frangopol 1998) is performed.

Serviceability Using AASHTO Specifications

For steel girders, serviceability condition with respect to permanent deformation under overload has to be checked. AASHTO states that for composite steel beams, the stress caused by nominal dead loads D_l plus 1.30 times the live load shall not exceed 95% of the specified minimum yield strength of steel F_y (to control yielding of steel structures and slip of slip-critical connections due to vehicular live load). For noncomposite section, this stress should not exceed 80% of F_y. These considerations are used in the following to determine serviceability limit state function using moment in critical section as Akgül and Frangopol (2004) proposed. The formulations presented in this paper focus on steel girders only; serviceability of the concrete deck based on deflection, cracking, and delamination are excluded. The steel section S_2 that is analyzed herein is noncomposite and was found to be noncompact. Therefore, the maximum flexural strength of the steel composite section cannot be computed as the resultant moment of the fully plastic stress distribution because the steel section will fail with local web buckling. The flexural capacity of the steel section is computed using the composite section modulus S_{bc}. The moment caused by the nominal dead load plus the live load shall not exceed 80% of the moment at first yielding in the section (as explained previously for a noncomposite section). Therefore, the limit state equation for serviceability of a steel girder i at critical moment section S_2 is

$$g_i = 0.80F_yS_{bc} - (M_{\mathrm{DLNC},i} + M_{\mathrm{DLC},i} + M_{LL,i}) \tag{5}$$

where $M_{\mathrm{DLNC},i}$, $M_{\mathrm{DLC},i}$, and $M_{LL,i}$=moment in girder i due to noncomposite and composite dead loads, and due to live load, respectively. It is noted that $M_{DNLC,i}$ is the moment due to noncomposite dead load (due to steel) that is multiplied by the coefficient λ_s (Table 1) to take into account the uncertainty on the steel weight. The composite dead load in a noncomposite section (denoted as η_1) consists of a uniform dead load component w_{DLC} (including dead loads due to the slab, asphalt, pavement, curbs, railings, and utility piping, respectively) and a concentrated dead load compo-

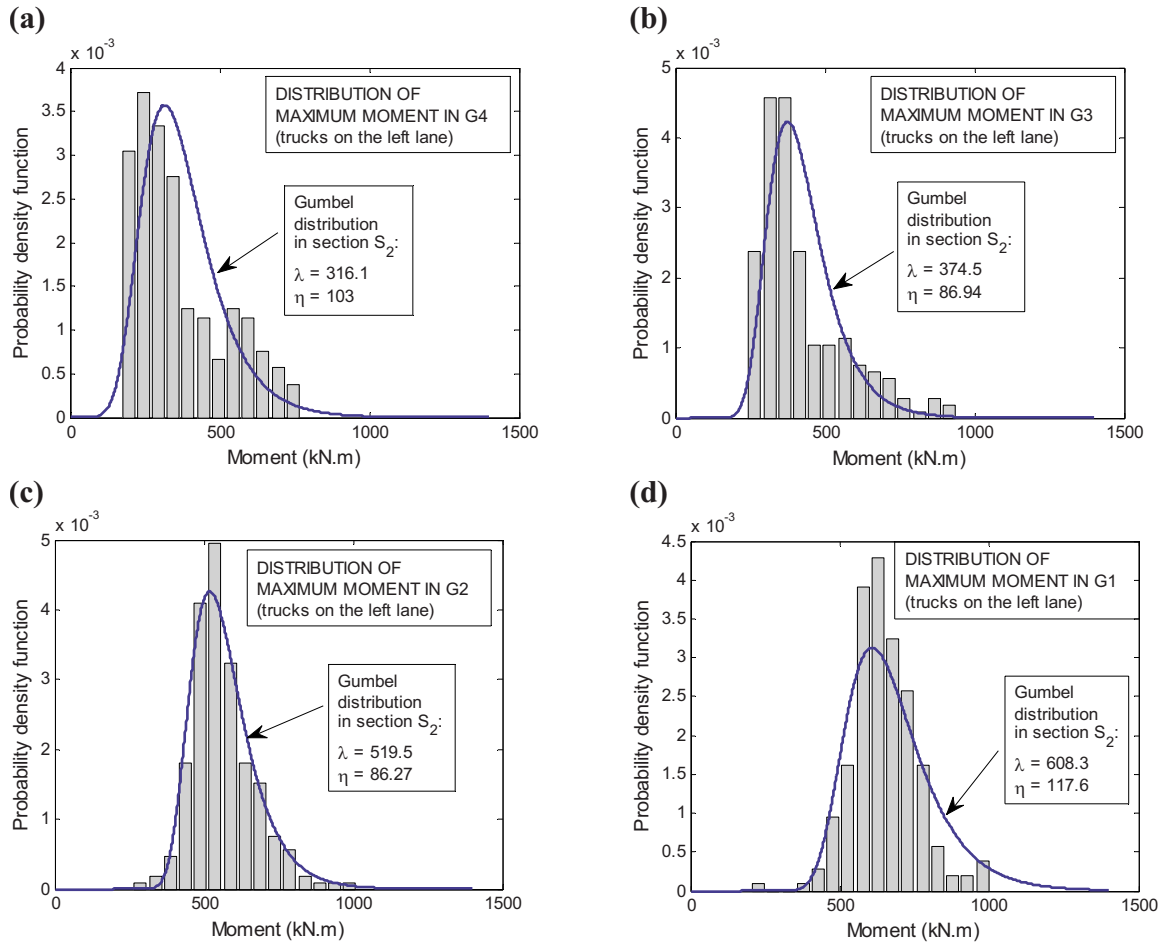

Fig. 11. Distribution of maximum moment in section S_2 (for trucks on the left lane) in: (a) G4; (b) G3; (c) G2; and (d) G1

nent P_{DLC} due to steel diaphragm and splice loads (Akgül and Frangopol 2004). η_1 includes the moments due to these separate loads. η_2 and η_3 are the moment values corresponding to w_{DLC} and P_{DLC}, respectively. Considering the uncertainty factor λ_s for P_{DLC}, the composite dead load moment is written as

$$M_{\mathrm{DLC},i} = \eta_2 + \eta_3\lambda_s = \eta_4 w_{\mathrm{DLC}} + \eta_3\lambda_s \tag{6}$$

where $\eta_4 = \eta_2 / w_{\mathrm{DLC}}$. The uniform dead load is expressed as the sum of the load due to the slab, the asphalt, the curbs, the railings, and the utility piping as

$$w_{\mathrm{DLC}} = w_{sl}\lambda_c + \frac{t_a b_a \gamma_a \lambda_a}{N_G} + \frac{2t_c b_c \gamma_c \lambda_c}{N_G} + \frac{2w_r}{N_G} + w_{pG} \tag{7}$$

where t and b=thickness and width of an individual component (with subscript *sl* for slab, *a* for asphalt, *c* for curbs, *r* for railing, *p* for utility piping, respectively); γ_a, γ_c=asphalt and concrete unit weight; N_G=number of girders; and the subscript G denotes that the piping weight is per girder. The values of $M_{\mathrm{DLC},i} + M_{\mathrm{DLNC},i}$, in each section of the two first spans of the I-39 Bridge, are shown in Fig. 12(a) for interior and exterior girders. In this study, the deterioration of steel girders is based on the salt water exposure and atmospheric corrosion of structural metal. Corrosion reduces the original thickness of the webs and flanges of these girders. Corrosion is assumed to penetrate the top and sides of the bottom flanges, in addition to each side of the web. It is considered that the exposure to leaking salt water is heavy at supports (e.g., section S_2 for I-39 Bridge) and that corrosion occurs throughout the web height. A power function for the corrosion model is used (Townsend and Zoccola 1982; McCuen and Albrecht 1994) $p = b_0 t^{b_1}$, where b_0 and p is the corrosion losses after one and t years, respectively, and b_1 is the slope of the logarithmic transformation of p. A rural-urban area is considered for the I-39 Bridge. Parameters b_0 and b_1 follow lognormal distribution with mean and standard deviation $(\mu;\sigma)$ equal to (32.07;2.89) and (0.5;0.045), respectively (Akgül and Frangopol 2004). The section modulus is the only parameter of girders that is affected by corrosion. Monte Carlo simulations are performed to find the evolution of the mean and the standard deviation of this parameter with time.

The moment due to live load is

$$M_{LL,i} = D_f^i (M_{la,i}^{S_2} + I_f M_{trk,i}^{S_2}) \tag{8}$$

where $I_f = 1 + IM$ and IM=dynamic load allowance fixed at 33% and $M_{la,i}^{S_2}$, $M_{trk,i}^{S_2}$=moment $M_{la,i}$ (90% of the moment associated with a design lane load) and moment $M_{trk,i}$ (90% of the moment associated with two design trucks) in section S_2, respectively. Indeed, for an interior pier, 90% of the effect of two design trucks spaced by 15,000 mm between the lead axle of one truck and the rear axle of the other truck ($M_{trk,i}$) are combined with $M_{la,i}$ =90% of the effect of a design lane load (9.3 N/mm uniformly distributed in the longitudinal direction) as specified in AASHTO (2007). It is noted that the two design trucks have two 145 kN axles and one 35 kN axle with spacing fixed at 4300 mm between each axle. These trucks are placed on the two spans to compute

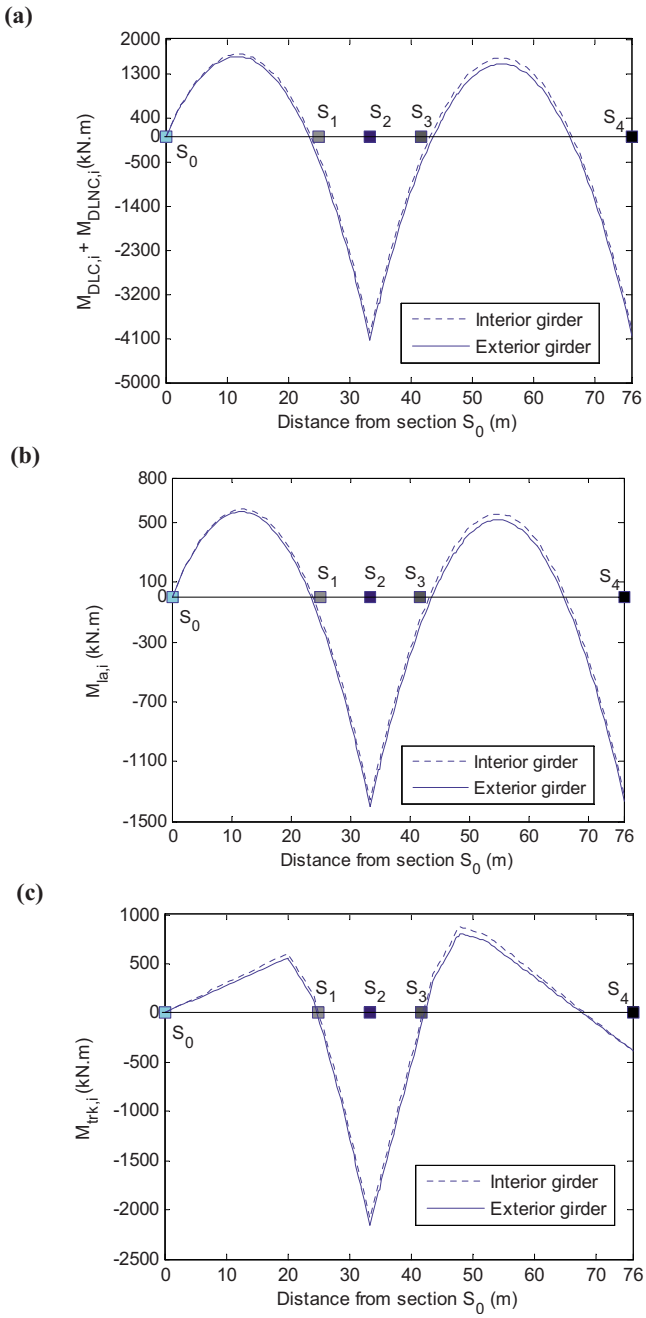

Fig. 12. (a) Moment due to dead loads ($M_{\mathrm{DLC},i}+M_{\mathrm{DLNC},i}$); (b) 90% of the moment due to one design lane load ($M_{la,i}$); and (c) 90% of the moment associated with two design trucks placed to obtain the highest moment in section S_2($M_{trk,i}$), for interior and exterior girders in the two first spans of the I-39 Bridge

the highest moment in section S_2 and a dynamic allowance is associated with $M_{trk,i}^{S_2}$, as detailed in Eq. (8). The values of $M_{la,i}$ and $M_{trk,i}$, in each section of the two first spans of the I-39 Bridge, are shown in Figs. 12(b and c), respectively, for interior and exterior girders.

The DF D_f^i (calculated for each girder i) depends on several criteria, among which the type of deck and girders, the number of design lanes loaded, the span length, the transverse girder spacing, the stiffness of the member, and whether the girder is an exterior or interior girder. The DF D_f^{int} for interior girders is expressed as

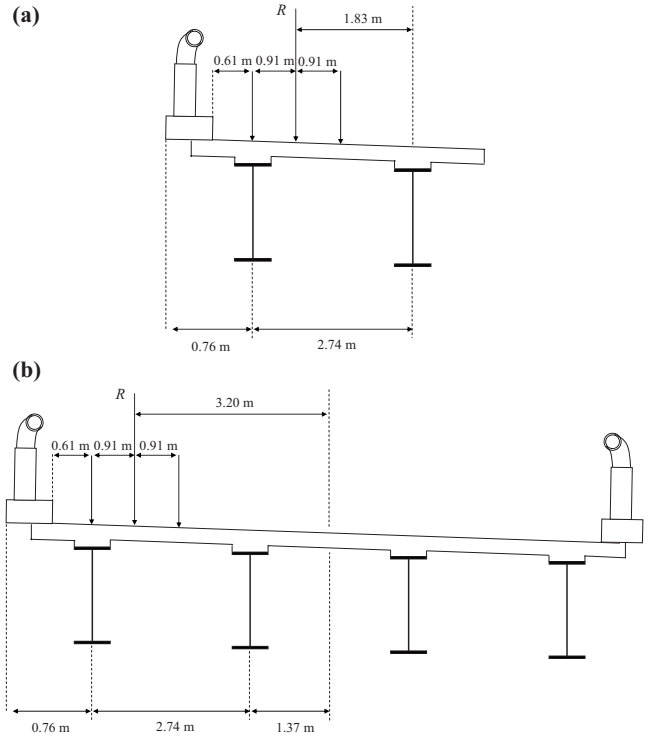

Fig. 13. Exterior girder DF determined by: (a) level rule; (b) a special analysis proposed in AASHTO (2007)

$$D_f^{\mathrm{int}} = 0.06 + \left(\frac{S}{4300}\right)^{0.4}\left(\frac{S}{L}\right)^{0.3}\left(\frac{K_g}{Lt_s^3}\right)^{0.1} \quad \text{with} \quad K_g = n(I + Ae_g^2) \tag{9}$$

where L=length of the span if the region is in positive flexure and average of the length of the two adjacent spans if the region is in negative flexure [see Fig. 12(a) for the moment due to the dead loads]; S=girder spacing; n=modular ratio; e_G=distance from the centroid of the steel girder to the midpoint of the concrete deck; A=cross-sectional area of the steel girder; I=moment of inertia of the steel girder. Eq. (9) is considered in sections S_1 and S_2; and the DF is assessed at 0.49 in both sections for interior girders (G2 and G3). It is noted that the multiple presence factor is not applied in case of interior girders since this parameter was already considered to determine the formula in Eq. (9). However, it is noted that the bridges considered in the development of Eq. (9) had interior end diaphragms only (i.e., no interior diaphragms within the spans). If interior diaphragms are provided within the spans (as in the case of I-39 Bridge in sections S_1 and S_2), AASHTO (2007) recommends to use computer programs, such as finite difference method, finite-element method, methods based on the formation of plastic hinges, among others, to increase the accuracy of the structural analysis. Using in situ information provided by SHM to calibrate structural parameters is then justified in this context of uncertainty. To compute the DF D_f^{ext} for exterior girders when one lane is loaded, the lever rule is generally applied (according to AASHTO specifications). The lever rule involves the use of statics to determine the wheel-load reaction at the exterior girder by summing moments about the adjacent girder, assuming the concrete deck is hinged at the interior girder [see Fig. 13(a)]. This enables to assess the distribution factor at $(1.83/2.74)\times 1.2=0.80$ for exterior girders (G4 and G1), by considering the multiple presence factor of 1.2. However, the lever

rule does not consider diaphragm or cross frames (which are present in sections S_1 and S_2, see Fig. 1). The presence of these elements makes the cross section deflecting and rotating as a rigid cross section. AASTHO proposes an interim provision until better methods of calculation are provided. In this case, the reaction R on exterior beam in terms of lane is expressed as

$$R = \frac{N_l}{N_b} + \frac{X_{\text{ext}} \sum_{N_l} e}{\sum_{N_b} x^2} \tag{10}$$

where N_l=number of loaded lanes under consideration; e =eccentricity of design truck or a design lane load from the center of gravity of the pattern of girders; x=horizontal distance from the center of gravity of the pattern of griders to each girder; X_{ext}=horizontal distance from the center of gravity of the pattern of girders to the exterior girder; and N_b=number of girders. For one loaded lane on the Wisconsin Bridge [see Fig. 13(b)], R is assessed using Eq. (10). R is finally multiplied by the multiple presence factor m=1.2, and the DF for exterior girders (G4 and G1) is 0.72. This method of calculation is chosen in the following instead of the lever rule that does not consider the presence of cross frames. It is obvious that evaluating directly the DF by using in situ tests can decrease dramatically all the uncertainties related to this coefficient.

Random variables and deterministic parameters selected in this study are indicated in Fig. 3. All random variables are assumed to have lognormal distribution and are characterized by their mean value μ and standard deviation σ. Random variables associated herein to a steel girder in section S_k are F_y, λ_a, λ_c, λ_s, S_{bc}, $M^{S_k}_{la,i}$, $M^{S_k}_{trk,i}$, I_f, and D^i_f. Descriptions of these random variables and the deterministic parameters are provided in Tables 1 and 2, respectively. The reliability index profile [associated with Eq. (5) in section S_2] that considers the corrosion effects and the AASHTO DFs is shown in Figs. 14(a–e) for girder G1 (D_f^{G1}=0.72), G2 (D_f^{G2}=0.49), G3 (D_f^{G3}=0.49), G4 (D_f^{G4}=0.72), and for the series system, respectively. Northbound Wisconsin Bridge is modeled herein, considering that failure of any girder causes the bridge failure (even if single-girder failure does not necessary cause bridge failure, due to redundancy). All four girders are considered in series and the system reliability index is associated with the mean of the Ditlevsen's bounds of probability of failure (Ditlevsen 1979). It is noted that the initial time in this figure is the time when the bridge was built. The reliability is then assessed from the beginning of the life of the structure until the end of the service life (75 years after construction).

DFs for girders G1, G2, G3, and G4 are now updated at year 43 for each girder using crawl test results. It is noted that DFs determined in section S_1 are used in section S_2 with the assumption that they do not change significantly between these two sections as it was observed in Eq. (9) when considering AASHTO coefficients. Besides, girders G3 and G4 were instrumented in sections different from section S_1 (section S_3 in Fig. 1) and it was possible to check that the DFs obtained from controlled load tests were the same as those found in section S_1 for these two girders, respectively. The highest values of DFs obtained in Figs. 6 and 7, when the truck is on the right or on the left lane, are considered for each girder. The new DFs after year 43 are then 0.52, 0.56, 0.56, and 0.54 for girders G1, G2, G3, and G4, respectively (after applying the multiple presence factor, as explained previously). For some components like girders G1 and G4, SHM data used at year 43 decreases the initial value of the DF and there is, therefore, an increase in the reliability index at year 43 [see Figs. 14(a and d)]. Conversely, for interior girders G2 and G3, the DF calculated from crawl tests is higher than the one given by AASHTO codes and there is a decrease of the reliability index at year 43 [see Figs. 14(b and c)]. Finally, the slope of the reliability index profile for the system is slightly larger after calibrating DFs at year 43 [Fig. 14(e)].

Serviceability Including SHM Results

A different approach to quantify the serviceability performance of the structure is proposed herein. This approach uses data from the long-term SHM program, conducted from August 12th to November 3rd 2004 (Mahmoud et al. 2005). Long-term SHM allows to approach the extreme moment due to heavy trucks. A time-variant function $\varsigma(t)$ at the critical location S_2 is introduced, which is used to predict future M_{traffic} through the probability distributions of the extreme values, such as Gumbel, Fisher-Tippett, or Weibull. Such a function was introduced by Liu et al. (2009a,b) to predict future extreme values of stresses. The histograms of moment that have been computed in section S_2 for the four girders G1, G2, G3, and G4, when trucks are on the right lane (Fig. 10) or on the left lane (Fig. 11) have enabled to determine the best fitting values of the Gumbel distribution introduced in Eq. (4). Thus, the extreme values of the SHM data in the future, $M_\chi(T)$ can be predicted as

$$M_\chi(T) = \lambda - \eta \ln\left[-\ln\left(1 - \frac{1}{T}\right)\right] \tag{11}$$

where T=return period. In the following, only the worst case of loading (truck moving through the bridge on the right or on the left lane) is considered for each girder. Obviously, the worst case for girders G2 and G1 is when trucks are on the left lane [compare Figs. 11(c) and 10(c) for G2 with Figs. 11(d) and 10(d) for G1, respectively]. For girders G4 and G3, the worst case is when trucks are on the right lane [compare Figs. 11(a) and 10(a) for G4 with Figs. 11(b) and 10(b) for G3, respectively]. The moment in girder i due to traffic, $M^i_{\text{traffic}}(t)$ at time t, is then expressed as

$$M^i_{\text{traffic}}(t) = \varsigma(t) M_\chi \tag{12}$$

where

$$\varsigma(s, t=T) = \max\left(\frac{M_\chi(T)}{\max(M_1, M_2, \ldots, M_k)}; 1\right) \tag{13}$$

The expression of the serviceability limit state function introduced in Eq. (5) is reformulated for each girder i by introducing the moment $M^i_{\text{traffic}}(t)$ as follows:

$$g_i^* = 0.80 F_y S_{bc} - [M_{\text{DLNC},i} + M_{\text{DLC},i} + M^i_{\text{traffic}}(t)] \tag{14}$$

This new limit state function enables to consider both dead loads according to AASHTO specifications along with live loads that are directly found by SHM results. It is noted that there is no consideration of DF anymore within the limit state function g_i^* in Eq. (14) [compared to limit state function g_i in Eq. (5)], since the moment is directly assessed for each girder from monitoring results. The reliability index profile is shown for the four girders and the system (mean of the Ditlevsen's bounds for a system with components in series) in Fig. 15(a) when corrosion of steel girders is not considered, and in Fig. 15(b), when corrosion is introduced. It is obvious from these two figures that corrosion affects dramatically the reliability index profile of both components and system. The reliability indices shown in Figs. 15(a and b) are all larger than those in Fig. 14. Indeed, serviceability limit state func-

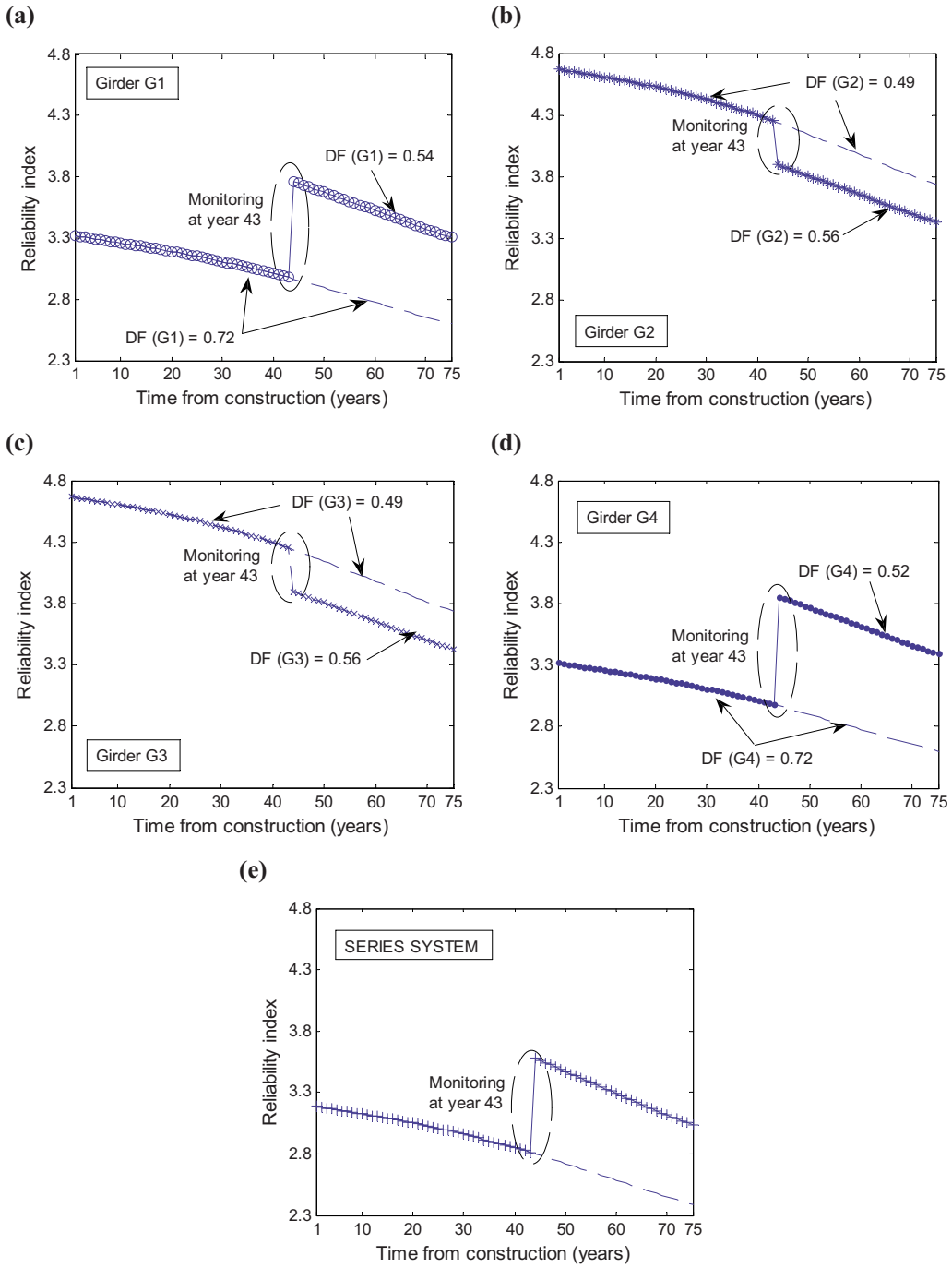

Fig. 14. Serviceability reliability index profile (associated with the limit state function of Eq. (5), and with considering corrosion) that uses AASHTO specifications by including or not including new DFs at year 2004: (a) for girder G1; (b) for girder G2; (c) for girder G3; (d) for girder G4; and (e) for the system

tion of Eq. (14) is associated with real traffic data (from August 12th to November 3rd 2004), whereas that of Eq. (5) is associated with a critical traffic configuration that produces the highest moment value in section S_2 according to AASHTO (2007). The former provides information on structural performance of the structure under real traffic whereas the latter quantifies the structural performance associated with a critical loading pattern configuration, used in design specifications. Finally, inclusion of the long-term SHM enables to compute a global reliability analysis that combines a classical approach with new information obtained from SHM.

Conclusions

In this paper, a practical approach to perform a reliability analysis of composite steel girders with respect to serviceability including information obtained from SHM is presented. The aim is to use available information and to complete the structural analysis that was initially performed. The information is used to update limit state functions, which improves the accuracy of both the structural and the reliability analyses. The proposed approach was applied by using the monitoring data collected on an existing bridge in Wisconsin. The following conclusions can be drawn:

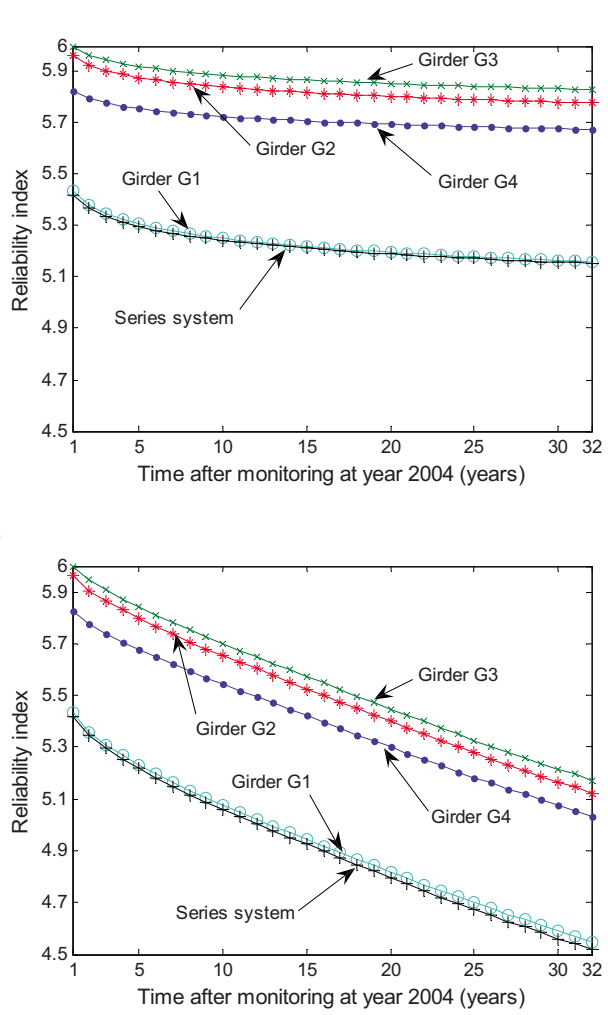

Fig. 15. Serviceability reliability index profile [associated with the limit state function of Eq. (14)] for girders G1, G2, G3, and G4 and for the series system, after monitoring at year 2004, by using AASHTO specifications and SHM results: (a) without considering corrosion; (b) with considering corrosion

1. The information obtained at some locations of the structure allows assessing the response of the structure at different locations. Two types of SHM results are used herein: the crawl tests that allow updating the DFs in each girder of the bridge, and the long-term monitoring program that provides additional information on the structural response of the bridge to traffic. These two types of information are then used in limit state equations. They both modify the parameters associated with serviceability limit state function;
2. It is noted that the two considered sections (i.e., the one where sensors are installed and the one where the structural analysis is performed) are not too far from each other. This justifies the use of the same DFs in these two sections and of the method to find histograms for moment in one section from those in another section. It is also noted that the analysis is conducted when only one lane is loaded and that conclusions depend obviously on the loading case;
3. Through the example presented in this paper, it is shown how to efficiently integrate SHM information in a structural reliability analysis. However, there is a strong need to generalize these concepts such that they can be applied for various types of bridges. Also, it is noted that the development of practical numerical models that are able to describe accurately the static and dynamic response of bridges while being computationally affordable for everyday practitioners still remains a challenge and requires future researches; and
4. The proposed approach can be used in a framework to include the SHM in a life-cycle cost performance context. The next step is to include SHM in a general framework at the scale of the entire bridge, where maintenance and repair strategies of the structure are optimized. Steps in this direction are already in progress (Frangopol and Messervey 2009a).

Acknowledgments

The support from (a) the National Science Foundation through Grant No. CMS-0639428, (b) the Commonwealth of Pennsylvania, Department of Community and Economic Development, through the Pennsylvania Infrastructure Technology Alliance, (c) the U.S. Federal Highway Administration Cooperative Agreement through Award No. DTFH61-07-H-00040, and (d) the U.S. Office of Naval Research through Contract No. N-00014–08-0188 is gratefully acknowledged. The writers want to express their profound thanks to Mr. Ian Hodgson, Lehigh University, and thank him for his constructive comments and suggestions with respect to monitoring of bridges. They also want to thank Alberto Deco, Lehigh University, and Victor Voiry, IFMA, Aubière, France, for participating in calculations. The opinions and conclusions presented in this paper are those of the writers and do not necessarily reflect the views of the sponsoring organizations.

Notation

The following symbols are used in this paper:

A = cross-sectional area of the steel section;
A_i = weight of the ith axle;
b_s = effective width of the concrete deck;
b_0 = corrosion loss after 1 year;
b_1 = slope of the logarithmic transformation of p;
C_i = number of scans;
D_i = distance between axle i and the first axle of the vehicle;
D_f^i = distribution factor for component i;
E = error function;
e = eccentricity of design truck or a design lane load from the center of gravity of the pattern of girders;
e_g = distance between the centers of gravity of the beam and deck;
F_y = yield strength of steel girder;
$F(M_\chi)$ = cumulative distribution function of M_χ;
f = scanning frequency of data acquisition unit;
Gi = ith girder;
g_i = serviceability limit state function for component i;
g_i^* = serviceability limit state function, based on long-term monitoring, for component i;

I = moment of inertia of the section;
$\tilde{I}$ = influence ordinate;
$\tilde{\boldsymbol{I}}$ = vector of influence ordinates;
I_k = kth moment of inertia defined in Fig. 4;
$\mathrm{IL}_{s_k}^{\mathrm{ext}}$ = IL in section S_k for an exterior girder modeled with a finite-element model;
$\mathrm{IL}_{\mathrm{ct}(s_k)}^{i}$ = IL in section S_k for component i determined from the crawl test;
$\mathrm{IL}_{s_k}^{\mathrm{int}}$ = IL in section S_k for an interior girder modeled with a finite-element model;
$i_{k,\mathrm{ext}}$ = maximum absolute values of $\mathrm{IL}_{s_k}^{\mathrm{ext}}$;
$i_{k,\mathrm{int}}$ = maximum absolute values of $\mathrm{IL}_{s_k}^{\mathrm{int}}$;
L = span length;
$M_{\mathrm{DLC},i}$ = moment in section i due to composite dead loads;
$M_{\mathrm{DLNC},i}$ = moment in section i due to noncomposite dead loads;
$M_{LL,i}$ = moment due to live loads in component i;
$M_{la,i}$ = 90% moment associated with a design lane load;
$M_{la,i}^{S_k}$ = value of $M_{la,i}$ in section S_k;
$M_{\mathrm{traffic}}^{i}(t)$ = moment due to heavy traffic in component i;
$M_{trk,i}$ = moment associated with two design trucks;
$M_{trk,i}^{S_k}$ = value of $M_{trk,i}$ in section S_k;
$M_{trk,i}$ = Moment due to truck load;
$M_{\chi}(T)$ = extreme moment after return period T;
m = multiple presence factor;
N_b = number of girders;
N_l = number of loaded lanes under consideration;
n = modular ratio between beam and deck;
p = corrosion loss after t years;
r_{ext} = ratio between the absolute peak values of $\mathrm{IL}_{s_2}^{\mathrm{ext}}$ and $\mathrm{IL}_{s_1}^{\mathrm{ext}}$;
r_{int} = ratio between the absolute peak values of $\mathrm{IL}_{s_2}^{\mathrm{int}}$ and $\mathrm{IL}_{s_1}^{\mathrm{int}}$;
S = girder spacing;
S_{bc} = elastic section modulus;
T = return period;
t_s = depth of concrete slab;
$\boldsymbol{W}$ = matrix dependent on vehicle axle weights;
X_{ext} = horizontal distance from the center of gravity of the pattern of girders to the exterior girder;
x = horizontal distance from the center of gravity of the pattern of griders to each girder;
y_{bG} = distance between elastic neutral axis (NA) and the bottom of the flange of the girder;
γ_i = weighting factor;
$\gamma_{i,l}$ = weighting factor when the truck is on the left lane;
$\gamma_{i,r}$ = weighting factor when the truck is on the right lane;
η = scale parameters;
λ_a = asphalt weight uncertainty factor;
λ_c = concrete weight uncertainty factor;
λ_s = structural steel weight uncertainty factor;
ε = vector dependent on vehicle axle weights and measured load effect readings;
ν = speed of the vehicle;
σ_b = stress at the bottom flange of the girder; and
$\varsigma(t)$ = ratio between extreme moment after return period T and extreme moment at time t.

References

AASHTO. (2007). *AASHTO LRFD bridge design specifications*, 4th Ed., AASHTO, Washington, D.C.

Akgül, F., and Frangopol, D. M. (2004). "Lifetime performance analysis of existing steel girder bridge superstructures." *J. Struct. Eng.*, 130(12), 1875–1888.

Aktan, A. E., Catbas, N., Turer, A., and Zhang, Z. (1998). "Structural identification: Analytical aspects." *J. Struct. Eng.*, 124(7), 817–829.

Aktan, A. E., Farhey, D. N., Helmicki, A. J., Brown, D. L., Hunt, V. J., Lee, K.-L., and Levi, A. (1997). "Structural identification for condition assessment: Experimental arts." *J. Struct. Eng.*, 123(12), 1674–1684.

Anderson, T. W., and Darling, D. A. (1952). "Asymptotic theory of certain "goodness-of-fit" criteria based on stochastic processes." *Ann. Math. Stat.*, 23(2), 193–212.

Ang, A. H.-S., and De Leon, D. (2005). "Modeling and analysis of uncertainties for risk-informed decision in infrastructures engineering." *Structure and infrastructure engineering*, Vol. 1, Taylor and Francis, London, 19–31.

Ang, H.-S. A., and Tang, H. W. (1984). *Probability concepts in engineering planning and design*, Vol. 2, Wiley, New York.

Ditlevsen, O. (1979). "Narrow reliability bounds for structural systems." *J. Struct. Mech.*, 7(4), 453–472.

Douglas, B. M., and Reid, W. H. (1982). "Dynamic tests and system identification of bridges." *J. Struct. Eng.*, 108(10), 2295–2311.

Ellingwood, B. R. (2005). "Risk-informed condition assessment of civil infrastructure: State of practice and research issues." *Structure and infrastructure engineering*, Vol. 1, Taylor and Francis, London, 7–18.

Estes, A. C., and Frangopol, D. M. (1998). "RELSYS: A computer program for structural system reliability analysis." *Structure engineering and mechanics*, Vol. 6, Techno Press, Daejeon, South Korea, 901–919.

Frangopol, D. M., and Liu, M. (2007). "Maintenance and management of civil infrastructure based on condition, safety, optimization, and life-cycle cost." *Structure and infrastructure engineering*, Vol. 3, Taylor and Francis, London, 29–41.

Frangopol, D. M., and Messervey, T. B. (2009a). "Life-cycle cost and performance prediction: Role of structural health monitoring." *Frontier technologies for infrastructures engineering, Structures and infrastructures book series*, S.-S. Chen and A. H.-S. Ang, eds., Vol. 4, Chap. 16, CRC, Boca Raton, Fla., 361–381.

Frangopol, D. M., and Messervey, T. B. (2009b). "Maintenance principles for civil structures." *Encyclopedia of structural health monitoring*, Vol. 4, Chap. 89, C. Boller, F.-K. Chang, and Y. Fujino, eds., Wiley, New York, 1533–1562.

Frangopol, D. M., Strauss, A., and Kim, S. (2008a). "Bridge reliability assessment based on monitoring." *J. Bridge Eng.*, 13(3), 258–270.

Frangopol, D. M., Strauss, A., and Kim, S. (2008b). "Use of monitoring extreme data for the performance prediction of structures: General approach." *Engineering structures*, Vol. 30, Elsevier Science, New York, 3644–3653.

Gumbel, E. J. (1958). *Statistics of extremes*, Columbia University Press, New York.

Hess, P. E. (2007). "Structural health monitoring for high-speed naval ships." *Proc., 6th Int. Workshop on Structural Health Monitoring*, F.-K. Chang, ed., DEStech Publications, Lancaster, Pa.

Liu, M., Frangopol, D. M., and Kim, S. (2009a). "Bridge system performance assessment from structural health monitoring: A case study." *J. Struct. Eng.*, 135(6), 733–742.

Liu, M., Frangopol, D. M., and Kim, S. (2009b). "Bridge safety evaluation based on monitored live load effects." *J. Bridge Eng.*, 14(4), 257–269.

Mahmoud, H. N., Connor, R. J., and Bowman, C. A. (2005). "Results of the fatigue evaluation and field monitoring of the I-39 Northbound Bridge over the Wisconsin River." *ATLSS Rep. No. 05-04*, Lehigh Univ., Bethlehem, Pa.

Marsh, P. S., and Frangopol, D. M. (2007). "Lifetime multiobjective op-

timization of cost and spacing of corrosion rate sensors embedded in a deteriorating reinforced concrete bridge deck." *J. Struct. Eng.*, 133(6), 777–787.

McCuen, R. H., and Albrecht, P. (1995). "Composite modeling of atmospheric corrosion penetration data." *Application of accelerated corrosion tests to service life prediction of materials*, ASTM, West Conshohocken, Pa., 65–102.

MINITAB release 15 statistical software. (2007). Minitab Inc., State College, Pa.

Morassi, A., and Tonon, S. (2008). "Dynamic testing for structural identification of a bridge." *J. Bridge Eng.*, 13(6), 573–585.

Moses, F. (1979). "Weigh-in-motion system using instrumented bridges." *Transp. Engrg. J.*, 105(TE3), 233–249.

O'Brien, E. J., Quilligan, M. J., and Karoumi, R. (2006). "Calculating an influence line from direct measurements." *Proc. Inst. Civ. Eng.*, 159(BE1), 31–34.

SAP 2000. (2009). *Integrated software for structural analysis and design*, Computers & Structures, Berkeley, Calif.

Townsend, H. E., and Zoccola, J. C. (1982). "Eight-year atmospheric corrosion performance of weathering steel in industrial, rural and marine environments." *Atmospheric corrosion of metals*, ASTM, West Conshohocken, Pa., 45–59.